IOP Publishing Journal of Physics: Condensed Matter
J. Phys.: Condens. Matter **27** (2015) 256002 (6pp) doi:10.1088/0953-8984/27/25/256002

Study of the negative magneto-resistance of single proton-implanted lithium-doped ZnO microwires

I Lorite[1], C Zandalazini[2], P Esquinazi[1], D Spemann[1], S Friedländer[1], A Pöppl[1], T Michalsky[1], M Grundmann[1], J Vogt[1], J Meijer[1], S P Heluani[2], H Ohldag[3], W A Adeagbo[4], S K Nayak[4], W Hergert[4], A Ernst[5] and M Hoffmann[6]

[1] Institut für Experimentelle Physik II, University of Leipzig, Linnéstraße 5, D-04103 Leipzig, Germany
[2] Laboratorio de Física del Sólido, Dpto. de Física, FCEyT, Universidad Nacional de Tucumán, Argentina
[3] Stanford Synchrotron Radiation Lightsource, Stanford University, Menlo Park, CA 94025, USA
[4] Institute of Physics, Martin Luther University Halle-Wittenberg, Von-Seckendorff-Platz 1, 06120 Halle, Germany
[5] Max Planck Institute of Microstructure Physics, Weinberg 2, 06120 Halle, Germany
[6] Institute of Physics, Martin Luther University Halle-Wittenberg, Von-Seckendorff-Platz 1, 06120 Halle, Germany

E-mail: lorite@physik.uni-leipzig.de

Received 26 March 2015, revised 4 May 2015
Accepted for publication 8 May 2015
Published 5 June 2015

Abstract

The magneto-transport properties of single proton-implanted ZnO and of Li(7%)-doped ZnO microwires have been studied. The as-grown microwires were highly insulating and not magnetic. After proton implantation the Li(7%) doped ZnO microwires showed a non-monotonous behavior of the negative magneto-resistance (MR) at temperature above 150 K. This is in contrast to the monotonous NMR observed below 50 K for proton-implanted ZnO. The observed difference in the transport properties of the wires is related to the amount of stable Zn vacancies created at the near surface region by the proton implantation and Li doping. The magnetic field dependence of the resistance might be explained by the formation of a magnetic/non-magnetic heterostructure in the wire after proton implantation.

Keywords: ZnO, magnetism, interface

(Some figures may appear in colour only in the online journal)

1. Introduction

A large number of reports indicate that vacancies and/or the doping with non-magnetic ions play a main role in triggering defect-induced magnetism (DIM) in ZnO [1–6]. In particular, it has been shown experimentally and theoretically that in ZnO, Zn vacancies (V_{Zn}) are the main defect that, for a concentration of ~5%, can trigger magnetic order at temperatures $T \geqslant 300$ K [2, 7, 8]. It has been suggested that room temperature magnetic order is better stabilized by hole doping ZnO, arguing that holes mediate the long-range coupling between localized magnetic moments [9].

Previously, lithium, as an element that can be easily incorporated into ZnO, was already used to produce p-type ZnO [10, 11]. However, the efficiency of p-doping with Li is generally limited by the formation of compensating interstitials, the spontaneous formation of opposite-charged defects (e.g. cations or vacancies), which pin or may even decrease the Fermi energy. In this case there are not enough charge carriers generated at the working temperature, increasing strongly the resistivity of the material. The work in [8] characterized the existing defects in ZnO nanoparticles doped with different concentrations of Li and concluded that the observed magnetic order at room temperature is related to Li and Zn defects; in particular,

Li influences the formation and stabilization of Zn vacancies, generating the predicted *p*-type ferromagnetism [9].

In our previous report we presented evidence of the magnetic order of the ZLH wires only after H^+ implantation for a minimum Li concentration of 3% [12]. The observed magnetism is due to the spin polarization of the O–2p band. This spin polarization occurs due to the proximity to the magnetic moments at the Zinc vacancies. These are produced during H^+ implantation and stabilized thanks to the Li doping [12]. Therefore, the Li concentration fixes the amount of V_{Zn} large enough to produce magnetic order at room temperature.

We note that in general the main property used in the literature to prove the existence of DIM in ZnO is the bulk magnetization, even in small oxide structures such as ZnO nanorods [13] or ZnO nanoparticles [14]. However, in spite of the importance for the future miniaturization of spintronic devices with high-temperature magnetic order and low resistivities, evidence of ferromagnetic behavior at room temperature in a single micro- or nanostructure of ZnO has not been reported in the literature yet. The present work reports on the magneto-transport properties of low resistive Li-doped ZnO microwires after proton implantation. We believe that the observed transport properties are of interest for the development of spintronic devices based on these materials.

2. Experimental

ZnO and Li-doped ZnO microwires were prepared by a carbothermal process as explained elsewhere [12, 15]. The studied wires had a diameter of between ≃0.5 μm and ≃10 μm and a length of some ≃100 μm. The percentage of Li was chosen following previous reports [16–18]. The H^+ implantation of the ZnO microwires was performed in a remote hydrogen DC-plasma chamber in parallel-plate configuration for 1 h at a current of 60 μA [15, 19]. Assuming a displacement energy of 18.5 eV and 40 eV for Zn and O in pure ZnO lattice [20] SRIM simulation indicates that it is possible to create both V_{Zn} and O-vacancies (V_O) within the first 10 nm from the surface of ZnO due to the low energy of H^+ implantation used in this work.

The pure ZnO and ZnO:Li(7%) as well as H^+-implanted ZnO and ZnO:Li(7%) microwires are labeled ZnO, ZL, ZH and ZLH, respectively. Single microwires were selected using an optical microscope and fixed on a Si/Si_3N_4 substrate. The electrical contacts were done by clenching gold wires with indium on the microwire providing ohmic contacts at all measured temperatures. The magneto transport measurements were performed in a He-cryostat with the possibility of applying a magnetic field of 8 T at a maximum temperature of ≃250 K. The rotating sample holder allowed us measurements of the magneto transport properties at fields applied perpendicular and parallel to the electrical current direction, which is along the main axis of the wire.

Electron paramagnetic resonance (EPR) measurements were performed with a BRUKER EMX Micro X-band spectrometer at 9.41 GHz with an Oxford ESR 900 flow cryostat at temperatures from 6–300 K in the dark and under illumination with the full spectrum of a Xe-lamp. The sample volume was ≃15 mm^3 loosely packed ZnO microwires, previous to Li doping, in a standard test tube. EPR spectra were simulated by using the Easy Spin Matlab toolbox [21].

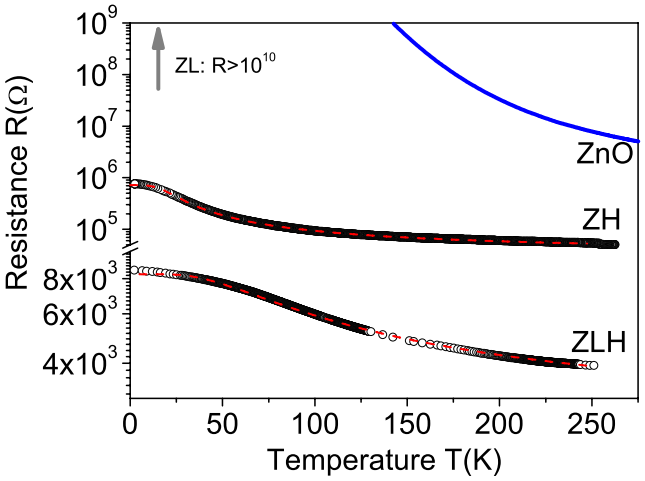

Figure 1. Resistance of all measured ZnO, ZH, ZL, and ZLH microwires of similar lengths and diameters (≃300 × 10 μm^2) as a function of temperature in a semi-logarithmic scale. The dashed red lines are the fittings of the experimental data to equation (1).

3. Results and discussion

Figure 1 shows the temperature dependence of the resistance of different ZnO wires with similar geometry. Pure ZnO wire shows a semiconducting-like behavior with $E_g \simeq 0.28$ eV obtained from the fit to equation(1) (R_s term). After doping with Li (ZL), the wire shows a highly insulating behavior having a resistance larger than $10^{10}\ \Omega$ (shown by an arrow in figure 1) at all temperatures. The highly insulating behavior of ZL is related to the carrier compensation by the complex formation of interstitial Li ions as donors with Li ions at Zn places as acceptors. The Zn vacancies act themselves as acceptors and could provide a p-type character to the wire [22].

After H^+ implantation the wires show a large decrease in the resistance of several orders of magnitude, see figure 1. As in the case of H^+ doped ZnO single crystals [19], the temperature (T) dependence of the ZLH and ZH microwires can be described using a simple parallel resistor model, considering two different contributions, namely: one with the typical Arrhenius dependence for semiconductors (R_s) and an activation energy E_g. The second one is given by a variable range hopping-like (R_{VRH}) mechanism that prevails at lower T. It is reasonable to assume that the VRH mechanism occurs mainly at the near surface region of the wire, whereas the bulk retains its thermally activated semiconducting behavior with the corresponding activation energy.

The equation for the total resistance based on the above described model can be written as:

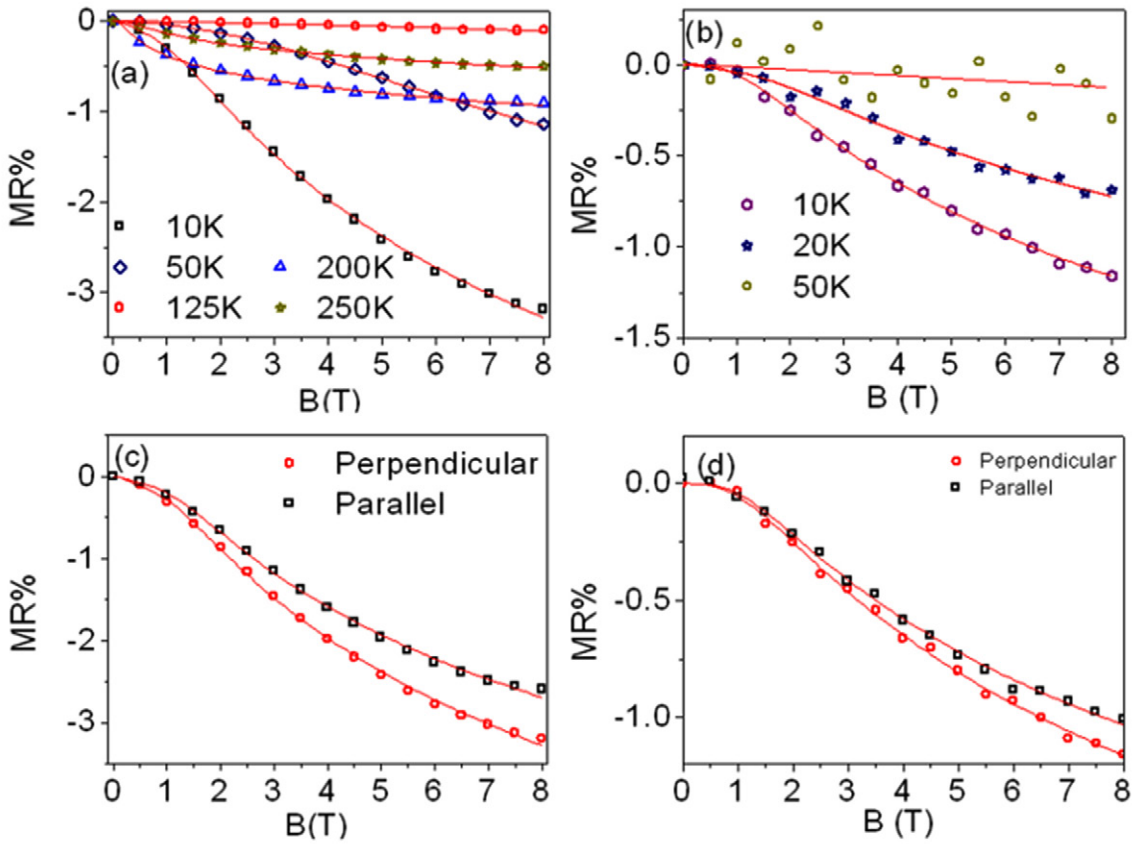

Figure 2. Magnetoresistance in perpendicular configuration at different temperatures of the ZLH (a) and ZH (b) microwires. (c) and (d) figures show a comparison of the magnetoresistance at 10 K for parallel and perpendicular configuration of ZLH (c) and ZH (d). All the continuous lines through the data are fits to equation (2).

$$R(T) = (R_s^{-1} + R_{\mathrm{VRH}}^{-1})^{-1} = \left[(R_1 \exp(E_g/2k_{\mathrm{B}}T))^{-1} + (R_2 \exp(E_n/T)^p)^{-1}\right]^{-1} \quad (1)$$

From the fits (dashed lines in figure 1) we obtain the following values for the ZH (ZLH) microwires: $R_1 = 46$ (3.5) kΩ, $E_g = 13$ (35) meV, $R_2 = 278$ (3) kΩ, and $E_n = 4$ meV and $p = 1/4$ for both. The large variation of the E_g from the undoped ZnO sample to the H^+ treated ones is related to the extra impurity band produced by the corresponding increase in the vacancies concentration and the hydrogen doping.

According to the fits the main difference between the ZH and ZLH wires is in the prefactor on the VRH part. This is because the H^+ implantation affects mainly the near surface region, as expected from the used implantation energy.

Figure 2 shows the magnetoresistance (MR) between 0 T and 8 T magnetic field applied perpendicular to the current flow or the *c*-axis of the ZLH (a) and ZH (b) microwires. Figures 2(c) and (d) show the MR for a field applied parallel and perpendicular to the *c*-axis of the ZLH and ZH microwires at different temperatures. The obtained results indicate: (1) For the ZLH microwire a negative MR (NMR) of −3.2% at 10 K (−0.5% at 250 K) is measured at 8 T applied field, see figure 2(a). (2) At the same applied field the ZH microwire presents a lower NMR of −1% at 10 K, being negligible above 50 K, see figure 2(b). (3) For the ZLH wire the NMR at a given fixed field is non-monotonous in temperature, see figure 3. (4) A comparison of the NMR between fields applied parallel and normal to the applied current (which has the same direction as the main axis of the wires) at 10 K, see figures 2(c) and (d), indicates that the (absolute) MR is smaller for parallel

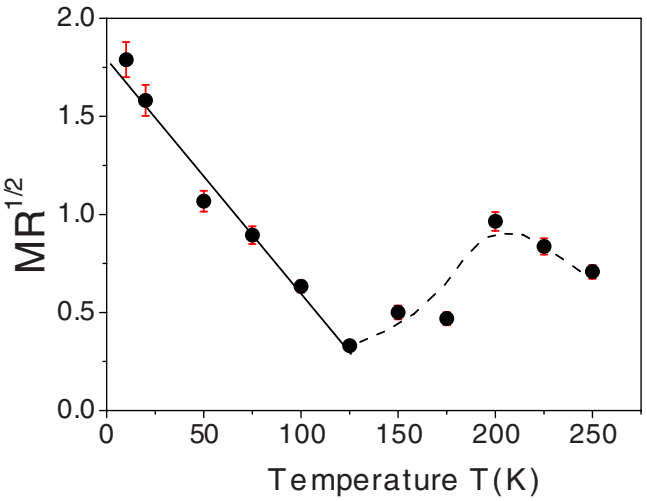

Figure 3. Square root of the absolute value of the magnetoresistance at a magnetic field of 8 T versus temperature for a single ZLH microwire. The solid and the dashed lines are only a guide for the eye.

fields than for fields applied normal to the current. The observed variation with the angle is compatible with the anisotropic MR, usually seen in ferromagnetic systems [23]. We found that the square root of the (absolute) MR of the ZLH microwire decreases linearly with temperature to 120 K, at higher temperatures the MR increases again showing a maximum at $T \sim 200$ K, see figure 3. The large and non-monotonous change of the MR with temperature is related to different transport contributions. In particular, the square temperature dependence of the MR below 120 K appears to be related to a mechanism occurring at the near surface region of the wire, where the VRH prevails. We stress that a similar behavior of the MR was observed in H^+ doped ZnO single crystals, but the minimum of the MR (at fixed field) occurred at $\simeq$40 K and the maximum at $\simeq$100 K, [19] instead of 125 K and 200 K as in our case, see figure 3. A possible origin of this effect is given below.

We describe the MR field dependence of the ZLH wire with a semi-empirical model proposed by Khosla and Fischer [24], widely used for magnetic transition metals in the past. The model takes into account two field-dependent contributions. The positive MR contribution with a quadratic field dependence at low fields and saturation at high fields (second term in the r.h.s. of equation (2)) is due to two conduction bands (usually s and d) with different conductivities. The negative MR one (first term in the r.h.s. of equation (2)) is attributed to a spin-dependent scattering between two sub-bands. Strictly speaking, it does not saturate at large fields, but its absolute value increases following a logarithmic field dependence. The semi-empirical formula is given by:

$$\frac{\Delta R}{R(0)} = -a^2 \ln(1 + b^2B^2) + c^2B^2/(1 + d^2B^2), \qquad (2)$$

where a, b, c and d are free parameters that depend on the carrier mobility, spin scattering amplitude, exchange integral conductivity and the spin of the localized moments; $R(0)$ is the resistance at zero field. The red lines in figure 2 follow equation (2) with the coefficients shown in figure 4 obtained from the fits.

In figure 4(a) the coefficients a, c, d and in figure 4(b) the coefficient b, obtained from the fits of equation (2) to the data of the ZLH wire, are shown. The parameters a and c decrease monotonously with the increase in temperature up to 150 K. Above this temperature they remain rather constant within the fitting error. The anomalous behavior in the MR is mainly reflected in the dependence of the fitting parameters b and to some extent in d, see figures 4(b) and (a). Following the original model [24] the parameter b should be inversely proportional to the temperature. This dependence is indeed observed in the temperature range where the VRH prevails, figure 4(b). However, this is not the case at higher temperatures. A simulation of the negative and positive contributions to the MR was done separately taking into account the obtained parameters, see figure 4(c). We observe that the positive MR contribution decreases monotonously with temperature. However, the negative MR presents the expected non-monotonous behavior

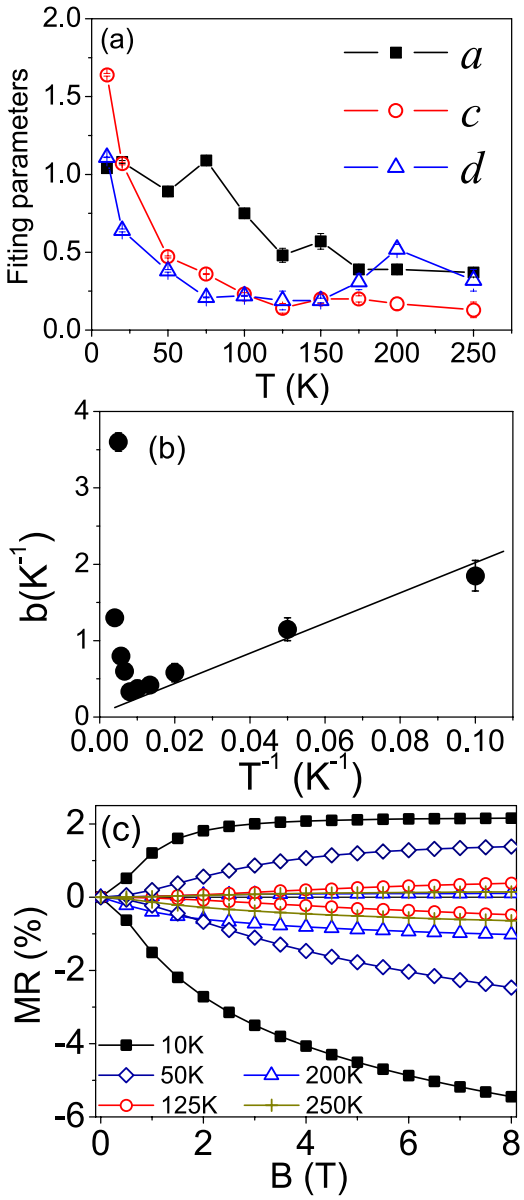

Figure 4. Coefficients a, c, d (a) and b (b) obtained from the fits to equation (2) of the data presented in figure 3 for the ZLH microwire. (c) The magnetoresistance calculated from the two contributions, the negative (the first term in equation (2)) and positive one (the second term in equation (2)), using the parameters of the fits.

in agreement with figure 3 and seems to be affected by two different contributions. The first one is active within the temperature range where the VRH mechanism overwhelms, i.e. below 150 K as the temperature dependence of the resistance suggests, see figure 1. The second one takes place once the carriers of the semiconductor are thermally activated, i.e. above 150 K.

Since for the ZnO microwire and after implantation of a comparable H^+ dose (ZH) there is a vanishing of the NMR at $T = 50$ K, see figure 2(b), it appears reasonable to assume that the density of V_{Zn} after implantation is smaller than that for ZLH. In order to clarify the origin for a possible decrease

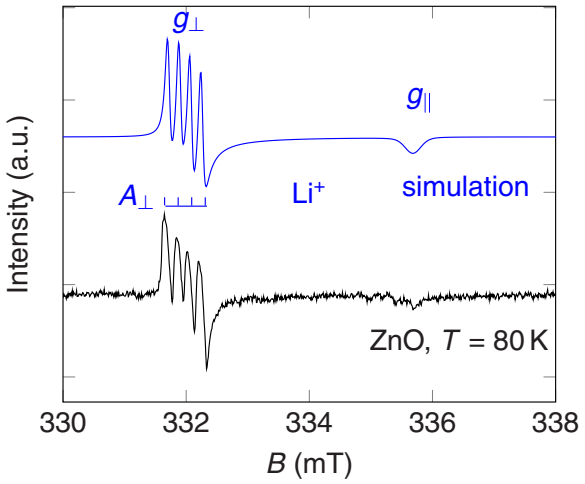

Figure 5. Experimental and simulated EPR spectrum of a $^{7}Li^{x}_{Zn}$ center found in the pure ZnO sample measured at 80 K with Xe-light illumination.

in the V_{Zn} concentration we have studied the agglomerate of ZnO microwires using EPR under UV-light to check for the possible existence of Li impurities, which can stabilize a small amount of V_{Zn}. Figure 5 shows, as an example, the signal obtained for ZnO recorded at 80 K under illumination. This temperature was selected due to the larger signal to noise ratio, taking into account that the EPR signal decreases with temperature [25]. The intense four-line spectrum at 332 mT is attributed to a $^{7}Li^{x}_{Zn}$ center with $S = \frac{1}{2}$ and $^{Li}I = \frac{3}{2}$ which can be described by a spin Hamiltonian with axial symmetry

$$\hat{H} = \beta(g_{\|}\hat{S}_z B_z + g_{\perp}[\hat{S}_x B_x + \hat{S}_y B_y]) + A_{\|}\hat{S}_z\, {}^{Li}\hat{I}_z + A_{\perp}(\hat{S}_x\, {}^{Li}\hat{I}_x + \hat{S}_y\, {}^{Li}\hat{I}_y) \quad (3)$$

where β is the Bohr magneton, $g_\perp$, $g_\parallel$, $A_\perp$ and $A_\parallel$ are the principal values of the Zeeman splitting tensor $\hat{g}$ and of the Li hf coupling tensor $\hat{A}$. The electron and nuclear spin operator components are denoted as $\hat{S}_i$ and $^{Li}\hat{I}_i$, respectively with $i = x, y, z$. The spin Hamiltonian parameters of the $^{7}Li^{x}_{Zn}$ center, $g_\parallel = 2.0028$, $g_\perp = 2.0251$, $A_\parallel = 0.1$ MHz, and $A_\perp = 5.1$ MHz as evaluated from the EPR spectrum shown in figure 5 are in good agreement with previously reported data of occupied Li acceptors in ZnO, where the Li^+ substitutes Zn^{2+} [26].

The obtained EPR signal reveals, therefore, the existence of Li impurities in nominally pure ZnO. Due to technical reasons is not possible, however, to use the absolute magnitude of the EPR signal to obtain a value of the Li content in the samples. These Li impurities will help to stabilize V_{Zn} after H^+ implantation. Since the concentration is small, the stabilized V_{Zn} concentration will be also small. This experimental result explains why magnetic order after implanting H^+ in ZH microwires is not observed, although a small NMR was observed at low temperatures.

As previously mentioned, two different contributions must take place in the observed field dependence of resistance. To account for the negative contribution within the VRH range, the model of static magnetic polaron [15, 27] may be used. According to this model, shallow donors form bound magnetic polarons which overlap to create a spin-splitting in the band. At higher temperatures, this contribution must be reduced and so the NMR, as observed. It has to be noted that for a small density of magnetic defects the VRH vanishes at the temperature of 50 K, as presented for ZH wire. However, this is not the case for ZLH, where the V_{Zn} density is enough to produce magnetic order within the 10 nm near surface region; meanwhile, the rest of the wire remains non-magnetic. The magnetic order only in the near surface region will produce, therefore, a DIM/non-DIM heterostructure. To explain the observed anomalous behavior in the NMR of ZLH, we have to consider the interface between magnetic and non-magnetic regions. With the rise in temperature, an increase in carrier concentration is produced. This increase in carriers may contribute to enhancing the DIM/non-DIM interfacial magnetism [28] at a certain temperature, i.e. 150 K–200 K, and so the spin polarization resulting in a more negative value of MR, see figure 3. This effect could help in the understanding and development of magnetic heterostructure for spintronic devices such as spin valves [29] through magnetic semiconductors.

4. Conclusions

In summary, the negative magnetoresistance of single H^+- and Li-doped ZnO microwires as well as the anisotropic magnetoresistance provide further evidence for the existence of magnetic order. The behavior of the magnetoresistance is non-monotonous with temperature. This behavior could be related to an enhancement of the spin polarization occurring at the interface between magnetic and non-magnetic regions of the proton implanted Li-doped microwires due to the increase in carrier concentration with temperature.

Acknowledgments

This work was partially supported by CIUNT under Grants 26/E439 and 26/E478, by ANPCyT-PICTR 35682, and by the Collaborative Research Center SFB 762 ‘Functionality of Oxide Interfaces’. We are grateful for the support within the DFG priority program SPP 1601 ‘New Frontiers in Sensitivity for EPR Spectroscopy’.

References

[1] Bhosle V and Narayan J 2008 *J. Magn. Magn. Mater.* **320** 983–9
[2] Khalid M *et al* 2009 *Phys. Rev.* B **80** 035331
[3] Ogale S B 2010 *Adv. Mater.* **22** 3125–55
[4] Stoneham M 2010 *J. Phys.: Condens. Matter* **22** 074211
[5] Volnianska O and Boguslawski P 2010 *J. Phys.: Condens. Matter* **22** 073202

[6] Esquinazi P, Hergert W, Spemann D, Setzer A and Ernst A 2013 *IEEE Trans. Magn.* **49** 4668–74
[7] Haug J, Chassé A, Dubiel M, Eisenschmidt C, Khalid M and Esquinazi P 2011 *J. Appl. Phys.* **110** 063507
[8] Awan S U, Hasanain S K, Bertino M F and Jaffar G H 2012 *J. Appl. Phys.* **112** 103924
[9] Peng H, Xiang H J, Wei S-H, Li S-S, Xia J-B and Li J 2009 *Phys. Rev. Lett.* **102** 017201
[10] Lee J, Cha S, Kim J, Nam H, Lee S, Ko W, Wang K L, Park J and Hong J 2011 *Adv. Mater.* **23** 4183–7
[11] Fan J C, Sreekanth K M, Xie Z, Chang S L and Rao K V 2013 *Prog. Mater. Sci.* **58** 874–985
[12] Lorite I *et al* 2015 *Appl. Phys. Lett.* **106** 082406
[13] Panigrahy B, Aslam M, Misra D S, Ghosh M and Bahadur D 2010 *Adv. Funct. Mater.* **20** 1161–5
[14] Li Z, Zhong W, Li X, Zeng H, Wang G, Wang W, Yang Z and Zhang Y 2013 *J. Mater. Chem.* C **1** 6807–12
[15] Lorite I, Esquinazi P, Zapata C and Heluani S P 2014 *J. Mater. Res.* **29** 78–83
[16] Chakraborti D, Narayan J and Prater J T 2007 *Appl. Phys. Lett.* **90** 062504
[17] Chawla S, Jayanthi K and Kotnala R K 2009 *Phys. Rev.* B **79** 125204
[18] Ran C J, Xu X G, Yang H, Wang Y, Miao J and Jiang Y 2012 *IEEE Trans. Magn.* **48** 3422–5
[19] Khalid M and Esquinazi P 2012 *Phys. Rev.* B **85** 134424
[20] Look D C, Hemsky J W and Sizelove J R 1999 *Phys. Rev. Lett.* **82** 2552
[21] Stoehr J and Siegmann H C 2006 *Magnetism—From Fundamentals to Nanoscale Dynamics* (*Springer Series in Solid State Sciences* vol. 152) (Berlin: Springer)
[22] Yi J B *et al* 2010 *Phys. Rev. Lett.* **104** 137201
[23] O'Handley R C 2000 *Modern Magnetic Materials* (New York: Wiley)
[24] Khosla R and Fischer J 1970 *Phys. Rev.* B **2** 4084–97
[25] Barzola-Quiquia J, Esquinazi P, Villafuerte M, Heluani S P, Poppl A and Eisinger K 2010 *J. Appl. Phys.* **108** 073530
[26] Schirmer O 1968 *J. Phys. Chem. Solids* **29** 1407–29
[27] Coey J M D, Venkatesan M and Fitzgerald C B 2005 *Nat. Mater.* **4** 173–9
[28] Quan Z, Zhang X, Liu W, Li X, Addison K, Gehring G A and Xu X 2013 *Appl. Mater. Interfaces* **5** 3607–13
[29] Tang J and Wang K L 2015 *Nanoscale* **7** 4325–37